Received: 5 April 2024 | Revised: 3 June 2024 | Accepted: 6 June 2024

DOI: 10.1111/pce.15008

ORIGINAL ARTICLE

Plant, Cell & Environment | PC&E | WILEY

# A synchronized, large-scale field experiment using *Arabidopsis thaliana* reveals the significance of the UV-B photoreceptor UVR8 under natural conditions

Susanne Neugart[1] | Viktoria Steininger[2] | Catarina Fernandes[2] | Javier Martínez-Abaigar[3] | Encarnación Núñez-Olivera[3] | Monika Schreiner[4] | Åke Strid[5] | András Viczián[6] | Andreas Albert[7] | Francisco R. Badenes-Pérez[8] | Antonella Castagna[9] | Beatriz Dáder[10] | Alberto Fereres[8] | Alenka Gaberscik[11] | Ágnes Gulyás[12] | Dylan Gwynn-Jones[13] | Ferenc Nagy[6] | Alan Jones[14,15] | Riitta Julkunen-Tiitto[16] | Nataliia Konstantinova[2] | Kaisa Lakkala[17] | Laura Llorens[18] | Johann Martínez-Lüscher[19] | Line Nybakken[20] | Jorunn Olsen[21] | Inmaculada Pascual[19] | Annamaria Ranieri[9] | Nicole Regier[22] | Matthew Robson[23,24] | Eva Rosenqvist[25] | Marco Santin[9] | Minna Turunen[26] | Filip Vandenbussche[27] | Dolors Verdaguer[18] | Barbro Winkler[7] | Katja Witzel[4] | Daniele Grifoni[28,29] | Gaetano Zipoli[30] | Éva Hideg[31] | Marcel A. K. Jansen[32] | Marie-Theres Hauser[2]

**Correspondence**
Éva Hideg, Ifjúság útja 6, Pécs, Hungary.
Email: ehideg@gamma.ttk.pte.hu

Marcel A. K. Jansen, Distillery Field, North Mall, Cork, Ireland.
Email: m.jansen@ucc.ie

**Funding information**
Ministry of Higher Education, Science and Innovation, Republic of Slovenia, Grant/Award Number: P1-0212; The Carl Trygger Foundation for Scientific Research, Sweden, Grant/Award Number: #CTS21:1666; Knowledge Foundation, Sweden, Grant/Award Number: #20130164; Swedish Research Council Formas, Sweden, Grant/Award Number: #942–2015–516; Faculty for Business, Science and Technology at Örebro University; Hungarian Scientific Research Fund, Grant/Award Numbers:

## Abstract

This study determines the functional role of the plant ultraviolet-B radiation (UV-B) photoreceptor, UV RESISTANCE LOCUS 8 (UVR8) under natural conditions using a large-scale 'synchronized-genetic-perturbation-field-experiment'. Laboratory experiments have demonstrated a role for UVR8 in UV-B responses but do not reflect the complexity of outdoor conditions where 'genotype × environment' interactions can mask laboratory-observed responses. *Arabidopsis thaliana* knockout mutant, *uvr8-7*, and the corresponding Wassilewskija wild type, were sown outdoors on the same date at 21 locations across Europe, ranging from 39°N to 67°N latitude. Growth and climatic data were monitored until bolting. At the onset of bolting, rosette size, dry weight, and phenolics and glucosinolates were quantified. The *uvr8-7* mutant developed a larger rosette and contained less kaempferol glycosides, quercetin glycosides and hydroxycinnamic acid derivatives than the wild type across all

For affiliations refer to page 13.

This paper is dedicated to Professor Gaetano Zipoli (1950–2019), an inspiring UV climatologist and a good friend.

OTKA, K-138022, K-132633; State Investigation Agency, Spain, Grant/Award Numbers: AGL2010-22196-C02-01, FPI BES-2011-045885; Spanish Government, Grant/Award Number: CGL2014-55976-R; Government of La Rioja, Grant/Award Number: "Afianza" 2023/05; Science Foundation Ireland, Grant/Award Numbers: 16-IA-4418, F3707, 267360, UV4growth; Austrian Science Fund (FWF); Academy of Finland; COST action FA0906

locations, demonstrating a role for UVR8 under field conditions. UV effects on rosette size and kaempferol glycoside content were UVR8 dependent, but independent of latitude. In contrast, differences between wild type and *uvr8-7* in total quercetin glycosides, and the quercetin-to-kaempferol ratio decreased with increasing latitude, that is, a more variable UV response. Thus, the large-scale synchronized approach applied demonstrates a location-dependent functional role of UVR8 under natural conditions.

**KEYWORDS**

flavonoid, glucosinolate, metabolite, plant morphology

## 1 | INTRODUCTION

The effects of light on plants are multifaceted, with light being both an important source of information and energy, as well as a potential stressor. Plants perceive the information content of light by sensing its spectral composition, intensity, photoperiod and direction. This information is used to steer growth and development (Chen et al., 2004; Chory, 2010; de Wit et al., 2016; Kami et al., 2010), including the biochemical make-up of the plant (Peters et al., 2018; Yang et al., 2018). There is ample evidence that ultraviolet-B radiation (UV-B; 280–315 nm) is, along with UV-A (315–400 nm), visible and far-red light, an important regulator of plant growth and secondary metabolite profiles. UV-B promotes UV protection and influences metabolism, development and plant defense (Demkura & Ballaré, 2012; Jenkins, 2009). Using classical indoor experiments, the UV-B photoreceptor, UV RESISTANCE LOCUS 8 (UVR8), has been identified and was found to mediate changes in gene expression, growth and development, morphology and stomatal function at low fluence rates of UV-B (Brown & Jenkins, 2008; Brown et al., 2005; Di Wu et al., 2012; Favory et al., 2009; Kliebenstein et al., 2002; Rizzini et al., 2011). Furthermore, UV-B induces accumulation of a set of metabolites protecting the sensitive macromolecules from the detrimental effects of UV, including flavonoids, terpenoids, alkaloids, glucosinolates, polyamines and tocopherols (Agati & Tattini, 2010; Hectors et al., 2007, 2014; Ibdah et al., 2002; Kusano et al., 2011; Schreiner et al., 2012; Stracke et al., 2010). It was also demonstrated that UVR8 mediates the accumulation of these metabolites by regulating key genes involved in their synthesis (Brown et al., 2005; Favory et al., 2009; Morales et al., 2013).

UVR8 is highly conserved, being present throughout the plant kingdom, as well as in green algae (Fernández et al., 2016), suggesting a critical, albeit largely unknown, function for plant life in the terrestrial environment (Findlay & Jenkins, 2016). Experiments performed in controlled chambers, greenhouses and/or sun simulators that used artificial UV sources revealed that *uvr8* mutants display a changed phenotype compared with their wild-type counterparts when exposed to UV-B radiation (Arongaus et al., 2018; Bernula et al., 2017; Besteiro et al., 2011; Brown et al., 2005; Demkura & Ballaré, 2012; Favory et al., 2009; Wargent et al., 2009). However, our knowledge of the functional role of UVR8 under natural solar conditions is rudimentary and is obtained from only a few studies that monitored growth and development of *uvr8* mutants outdoors for relative short periods (Coffey et al., 2017; Stockenhuber et al., 2024). It can be questioned whether there will be a discernable phenotype for *uvr8* mutants in the natural environment, given that the function of UVR8 is modulated by interactions with other photoreceptor signalling pathways, including the phytochrome and cryptochrome pathways (Huang et al., 2013; Mazza & Ballaré, 2015; Podolec & Ulm, 2018; Rai et al., 2019, 2020; Tissot & Ulm, 2020). For example, outdoor studies revealed the complex function of UVR8 in UV-A- and UV-B-driven signalling pathways (Morales et al., 2013), and the synergistic interaction of the cryptochrome- and UVR8-mediated molecular pathways in regulating acclimation to environmental stress conditions (Stockenhuber et al., 2024). At present, it is not known to what extent interactions with other environmental factors under outdoor conditions will mask UVR8 function. Most indoor studies have deduced the regulatory function of UVR8 under artificial conditions, often optimized for growth, and with a few hours a day of relatively high UV-B fluence rates in relation to low visible light. In contrast, the natural radiation environment is highly complex and characterized by rapid, and often unpredictable, changes in UV-B (Barnes et al., 2015, 2016; Moriconi et al., 2018). Furthermore, these changes in UV-B can be accompanied by equally rapid changes in other environmental parameters, including UV-A and total radiation, temperature and relative humidity. The effects of exposure to these environmental changes may mask any UVR8-mediated effect, or cause complex interactive effects, which may be synergistic, additive or antagonistic (Jansen et al., 2019). Indeed, recent studies have found that effects of UVR8 were limited to enhancement of accumulation of UV-absorbing pigments under wintery outdoor conditions where plants were exposed to natural UV-B irradiation (Coffey et al., 2017) or an increase of plant fitness and survival rate (Stockenhuber et al., 2024). Such a restricted role for UVR8 appears to contradict the evolutionary conservation of UVR8. Therefore, the overarching aim of this study was to analyse the functional role of UVR8 under a comprehensive range of complex, dynamic, natural environments that represent a natural gradient of UV irradiances. To this end, two genotypes that only differ in their functionality of UVR8

were cultivated outdoors at 21 locations throughout Europe. In this synchronized, genetic field perturbation experiment, we determined the importance of the UV-B receptor for growth, biomass production and accumulation of the UV-protecting pigments, flavonoids and glucosinolates. Collectively, our data reveal how UVR8 contributes to plant acclimation under ambient, natural environmental conditions.

## 2 | MATERIALS AND METHODS

### 2.1 | Geographic and meteorological conditions

A total of 21 European locations were selected along a latitudinal and longitudinal gradient (Figure 1 and Supporting Information S1: Table S1). These locations were ordered numerically from 1 to 21 along a latitudinal gradient from north Rovaniemi (Finland, 66.50°N) to south Xàtiva/Valencia (Spain, 38.99°N); a linear distance of over 3000 km. The longitudinal gradient was from Cork (Ireland, 8.49°W) to Joensuu (Finland, 29.77°E). This represents a substantial part of the natural distribution area of *Arabidopsis thaliana* in Europe. Geographic data (latitude and longitude) were combined with meteorological data. As temperature and light conditions are highly variable under outdoor conditions, we calculated the average temperature (AvTemp) from daily averages and defined maximal and minimal temperatures (daily maximum temperature [dMaxTemp], daily minimum temperature [dMinTemp]), and total radiation in MJ $m^{-2}$ $day^{-1}$ (Rad) over the period from sowing till harvest. Total radiation includes the UV-B, UV-A and PAR spectral regions. These data were collected from the closest weather station to the plants' cultivation site (Supporting Information S1: Table S1).

### 2.2 | Plant materials and genotypes

The original nonsense *uvr8-7* mutant in *Arabidopsis* accession Wassilewskija (Ws) (Favory et al., 2009) was backcrossed with Ws to remove the *proHY5:LUC* reporter. The F2 was selected for the absence of the hygromycin resistance associated with the reporter construct using both growth assays and polymerase chain reaction (PCR). The presence of F2 seedlings homozygous for the *uvr8-7* point mutation was determined by PCR and sequencing. For genotyping, DNA was extracted with the cetyltrimethylammoniumbromid method (Hauser et al., 1998) and used for a Web-based allele-specific PCR (Wangkumhang et al., 2007) assay with the following conditions: the PCR reaction contained 1 µL of DNA, 5 pmol of each primer (uvr8-7_5g63860mutF/uvr8-7_5g63860R for the mutant and uvr8-7_5g63860wtF/uvr8-7_5g63860R for the wild-type allele), 200 µM dNTPs and the 2× Accustart II PCR ToughMix (Quantabio) in a total reaction volume of 10 µL. The PCR conditions were an initial denaturation step of 3 min at 94°C and 35 cycles with 94°C/10 s, 63°C/15 s, 72°C/1 min, followed by the last extension phase at 72°C for 3 min. The amplicons were separated on 2% agarose gels. For sequencing, the PCR used the primers uvr8-7_5g63860R/5g63860uvr8-7F_T7 (Supporting Information S1: Table S2).

Seeds of both wild type and *uvr8-7* plants were collected from plants grown under the same conditions, at the same time, in the same laboratory. Also, seeds were harvested at the same time. After harvest, all seeds were after-ripened for 1 month at room temperature and the seed stocks were subsequently distributed to all the participating laboratories.

### 2.3 | Set-up of the synchronized genetic field perturbation experiment

At each of the 21 locations, ~400 seeds of each genotype were directly sown in trays containing prewetted soil, on the same day (7 April 2014) at all locations. Identical soil was used at all locations (Einheitserde ED63 T Profi substrate with natural clay (loam) and peat, pH 5.5–6.5, 90–270 mg/L nitrogen, 120–360 mg/L phosphorus, 120–360 mg/L potassium, obtained from Patzer GmbH and Co. KG). Similarly, identical trays (18 × 13.3 × 6.2 cm) were used at all locations. The trays contained ~1.2 L soil and had holes at 1.5 cm from the bottom for drainage. The surface of the trays was covered with cotton mesh (Muslin). At each location and for each genotype, four individual trays (replicates) were sown, with each tray containing 100 seeds. The trays were placed on brown cardboard (~10 cm extra cardboard around each of the trays) outdoors on tables, walls, terraces or roofs, to minimize access by herbivores. The places of the trays were chosen as to maximize the sky view factor to minimize unpredictable microclimatic effects. The trays were checked daily and watered when necessary. The eight trays were positioned in four groups of two, each group comprised both genotypes. Germination time, that is, first appearance of seedlings with visible cotyledons was recorded. When more than 50% of the seedlings of both genotypes had two true leaves the Muslin mesh was removed simultaneously from all trays. Seedlings were thinned at the four-leaf stage so that seedlings were about 2.0–2.5 cm apart and evenly distributed in the trays. Thinning was repeated if the rosettes started to overlap each other. Photographs of the trays were taken at the same time of the day, every week as well as at thinning and harvest (Figure 2). Photographs were used to follow the development of the rosettes as part of the quality control of the experiment. When at least three plants per tray started to bolt, that is, inflorescence buds were visible, the following actions were taken: (1) the rosettes were harvested at local noon (highest Sun position); (2) the number of days from sowing to harvest was recorded; (3) the number of plants per tray was noted; (4) fresh weight was determined and (5) the rosettes were frozen in liquid nitrogen. Rosettes from the same tray were pooled, lyophilized and sent to one common laboratory (Leibniz Institute) for metabolite analysis.

### 2.4 | Growth measurements

Growth measurements were all done in the same laboratory (Dept. of Applied Genetics & Cell Biology, University of Natural Resources & Life Sciences), using photographs taken by the different teams on each site. Photographs were taken perpendicular above each tray at

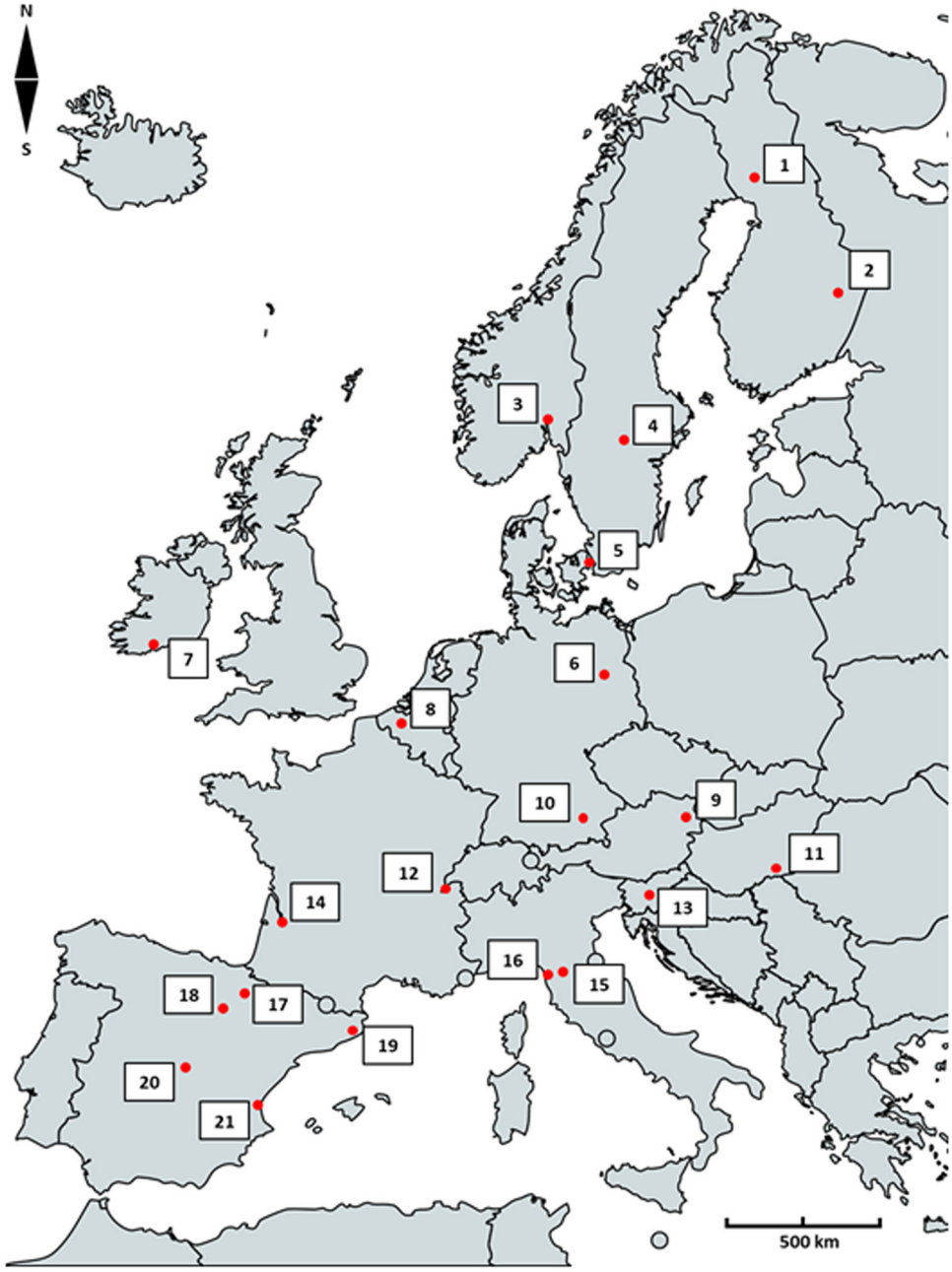


**FIGURE 1** Geographic location of the 21 European sampling locations used in this study. Red dots mark the sampling locations, numbered from north to south, Rovaniemi (1), Joensuu (2), Ås/Oslo (3), Örebro (4), Copenhagen (5), Grossbeeren (6), Cork (7), Ghent (8), Vienna (9), Munich (10), Szeged (11), Geneva (12), Ljubljana (13), Bordeaux (14), Florence (15), Pisa (16), Pamplona (17), Logroño (18), Girona (19), Madrid (20) and Xàtiva/Valencia (21). The map was created using mapchart.net. See Supporting Information S1: Table S1 for latitude and longitude data. [Color figure can be viewed at wileyonlinelibrary.com]

the time of thinning and at the onset of bolting. ImageJ software (Schneider et al., 2012) was employed to measure the radius of each rosette as the distance from the apical meristem to the tip of the three longest leaves and the average was calculated. All teams used the same trays and each image showed the full tray and a ruler as a scale for facilitating rosette size measurements. Dry weight (DW) per tray was determined using lyophilized material, and the overall weight was divided by the number of plants harvested per tray, to obtain the DW per plant. On average, 26 plants per tray were harvested thus the data presented correspond to about 105 plants per genotype and location and in total 4400 plants.

## 2.5 | Analysis of phenolic compounds

All phenolic compounds were analysed according to Neugart et al. (2015) with the following modifications. Lyophilized *Arabidopsis* leaf tissue (3–10 mg) was extracted with 600 µL of 60% aqueous

methanol in a thermoshaker for 40 min at 20°C. The extract was centrifuged at 41 000*g* for 10 min at the same temperature and the supernatant was collected in a reaction tube. This process was repeated twice with 300 µL of 60% aqueous methanol for 20 and 10 min, respectively; the three supernatants per sample were combined. The extract was evaporated under vacuum until it was dry and was then suspended in 200 µL of 10% aqueous methanol. The extract was centrifuged at 9259*g* for 5 min at 20°C through a Corning® Costar® Spin-X® plastic centrifuge tube filter (Sigma Aldrich Chemical Co.) for the high-performance liquid chromatography (HPLC) analysis. Each extraction was carried out in duplicate. Phenolic composition (hydroxycinnamic acid derivatives and flavonol glycosides) and contents were determined using a series 1100 HPLC (Agilent Technologies) equipped with a degaser, binary pump, autosampler, column oven, and photodiode array detector. An Ascentis® Express F5 column (150 mm × 4.6 mm, 5 µm, Supelco) was used to separate the compounds at a temperature of 25°C. Eluent A was 0.5% acetic acid and eluent B was 100% acetonitrile. The gradient used for Eluent B was 5%–12% (0–3 min), 12%–25% (3–46 min), 25%–90% (46–49.5 min), 90% isocratic (49.5–52 min), 90%–5% (52–52.7 min), and 5% isocratic (52.7–59 min). The determination was conducted at a flow rate of 0.3 mL $min^{-1}$ and a wavelength of, respectively, 320 and 370 nm for hydroxycinnamic acid derivates (HCA), and nonacylated flavonol glycosides. The HCA derivatives and all major flavonol glycosides were identified as deprotonated molecular ions and characteristic mass fragment ions according to Schmidt et al. (2010) and Saito et al. (2013) by HPLC–diode-array detection/electrospray ionization multistage mass spectrometry (HPLC-DAD-ESI-$MS^n$) using an Agilent series 1100 ion trap mass spectrometer in negative ionization mode. Nitrogen was used as the dry gas (10 L $min^{-1}$, 325°C) and the nebulizer gas (40 psi) with a capillary voltage of −3500 V. Helium was used as the collision gas in the ion trap. The mass optimization for the ion optics of the mass spectrometer for quercetin was performed at *m/z* 301 or arbitrarily at *m/z* 1000. The $MS^n$ experiments were performed in auto up to HPLC-DAD-ESI-$MS^3$ in a scan from *m/z* 200–2000. Standards (chlorogenic acid, quercetin 3-glucoside and kaempferol 3-glucoside; Roth) were used for external calibration curves.

## 2.6 | Glucosinolate analysis

Contents of all major glucosinolates in Arabidopsis rosettes were determined in the same laboratory as phenolic compounds, using a modified method according to DIN EN ISO 9167-1 (Wiesner et al., 2013). A sample of 5 mg of powdered plant material plus 100 µL of 0.1 mM 2-propenyl glucosinolate (BCR-367R, Community Bureau of Reference, Brussels) as the internal standard was extracted with 750 µL of 70% (v/v) methanol at 70°C. The preparation was boiled for 10 min and then centrifuged (2250*g*) for 5 min at room temperature. The supernatant was decanted and the residue was re-extracted twice with 500 µL of hot 70% methanol each time. The pooled extracts were loaded onto a mini column containing 500 µL of

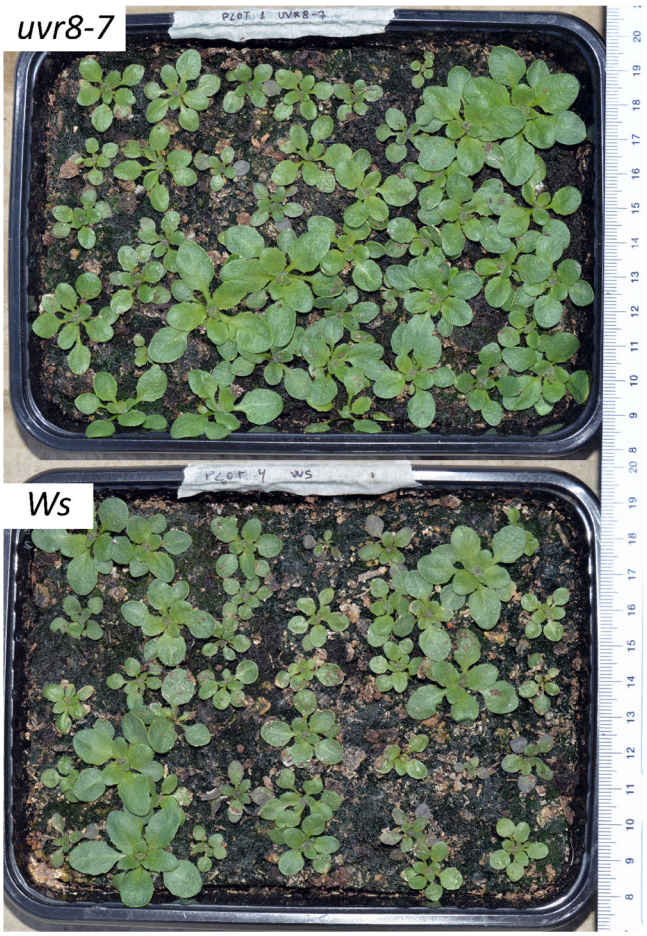


**FIGURE 2** A representative photo of trays from one location (Logroño) at harvest showing the two *Arabidopsis* genotypes used (top, *uvr8-7* mutant; bottom, Wassilewskija [Ws] wild type). [Color figure can be viewed at wileyonlinelibrary.com]

DEAD-Sephadex A-25 that had been conditioned with 2 M acetic acid and washed with 6 M imidazole formate. After loading, the column was washed with 0.02 M sodium acetate buffer. Finally, 75 µL of an aryl sulfatase solution (Sigma-Aldrich) was added and the preparation was incubated overnight. Desulfo-glucosinolates were eluted with water and analysed by HPLC using a Merck HPLC system (Merck-Hitachi) with a Spherisorb ODS2 column (Bischoff; particle size 5 µm, 250 mm × 4 mm). HPLC conditions were as follows: Solvent A, MilliQ water; Solvent B, 20% v/v acetonitrile in MilliQ water; Solvent C, 100% acetonitrile. The 60 min run consisted of 1% (v/v) B (2 min), 1%–20% (v/v) B (34 min), a 6 min hold at 20% (v/v) B, 20% B to 100% (v/v) C (2 min), a 5 min hold at 100% (v/v) C, 100% (v/v) C to 1% (v/v) B (2 min) and finally a 10 min hold at 1% (v/v) B. Separation and quantification were conducted at a flow rate of 0.7 mL $min^{-1}$ and a wavelength of 229 nm. Desulfo-glucosinolates were identified based on comparison of retention times and UV absorption spectra with those of known standards. Additionally, desulfo-glucosinolates were previously identified in *Brassica* species by HPLC-ESI-$MS^2$ using Agilent 1100 series (Agilent Technologies) in positive ionization mode (Krumbein et al., 2005;

Zimmermann et al., 2007). Glucosinolate content was calculated using 2-propenyl glucosinolate as an internal standard and the response factor of each compound relative to 2-propenyl glucosinolate (Brown et al., 2003).

### 2.7 | Statistical analyses

Exploratory data analysis found that the data did not meet all assumptions of normality (Shapiro–Wilk test) and homoscedasticity (Levene test), thus non-parametric tests (Kruskal–Wallis or Mann–Whitney) were used to test the effect of genotype. Spearman correlation coefficients ($r$) were used to examine the relationships between all the geographic, meteorological and physiological variables. Genotypes and locations were each described using different principal components analyses (PCAs). In the first PCA, the geographic, meteorological, and physiological variables were plotted. Among the physiological variables, growth (rosette size, DW), periods from sowing to germination and flowering, and content of each of the four metabolite families (glucosinolates, flavonol glycosides, anthocyanins and HCA derivatives) were used. For this purpose, metabolite families instead of individual compounds were selected because most compounds belonging to each family were significantly correlated. In the second PCA, only physiological variables were plotted, specifically growth variables and individual metabolite compounds. Thus, the influence of latitude and its correlated meteorological (temperatures, radiation) and developmental (periods from sowing to germination and harvest) variables was excluded. Statistical procedures were performed with either PAST (Hammer et al., 2001) or SPSS 24.0 for Windows (SPSS Inc.).

## 3 | RESULTS

### 3.1 | Geographical and meteorological variables

The 21 locations chosen are spread throughout Europe (Figure 1) and presented a broad range of meteorological conditions (Supporting Information S1: Table S1). The AvTemp during the cultivation period varied from 4.77°C to 18.43°C at the northern and southern extremes of the gradient, respectively (Locations 1 and 21). Total radiation (Rad) measured varied from 13.31 to 23.95 MJ $m^{-2}$ $day^{-1}$ between northern and southern locations. Overall, AvTemp, dMaxTemp, dMinTemp and Rad were significantly (at least $p < 0.05$) and negatively correlated with latitude (Figure 3). The distance and elevation difference between sampling locations and corresponding weather stations is relatively low (Supporting Information S1: Table S1), yet it is recognized that these differences may result in a slight mismatch between reported weather conditions and conditions experienced by the plants. However, against a backdrop of large latitudinal trends in temperatures and radiation we consider this discrepancy to be relatively minor (Supporting Information S1: Table S1). Furthermore, the impacts of possible microclimatic effects were reduced by growing wild type and uvr8-7 plants next to one another, and by standardizing all other materials for plant growth (see Section 2).

### 3.2 | Development and growth parameters

The period from sowing to germination for both genotypes varied between 4 and 32 days at Locations 21 and 2, respectively (Figure 1), while the period from sowing to flowering (harvest) varied between 23 and 57 days at Locations 21 and 1, respectively (Supporting Information S1: Table S3). Interestingly, the *uvr8-7* mutant had developed slightly larger rosettes than the wild type at the times of thinning and harvest (Figures 2 and 4, and Supporting Information S1: Table S3). The rosette DW at harvest showed a similar trend.

### 3.3 | Metabolite composition of the examined plant genotypes

A total of 21 abundant secondary metabolites were analysed in the wild type and *uvr8-7* above ground biomass: nine glucosinolates (five aliphatic and four indolic), four kaempferol glycosides, four quercetin glycosides, one anthocyanin, and three HCA derivatives (Supporting Information S1: Table S4). Chemical analysis of phenolic compounds by HPLC-$MS^n$ revealed the presence of the HCA derivative sinapoylglucoside as well as quercetin and kaempferol di- and triglycosides containing one rhamnose sugar moiety and quercetin and kaempferol di- and triglycosides with two rhamnose sugar moieties.

In plant material from all locations, and from both genotypes, the measured amounts of total glucosinolates were nearly eightfold greater than the total amount of phenolic compounds. Aliphatic glucosinolates were more abundant than indolic glucosinolates (84% vs. 16%, respectively, of total glucosinolates) (Figure 5 and Supporting Information S1: Table S4). Among phenolic compounds, kaempferol glycosides (representing 63% of total flavonoids) were more abundant than quercetin glycosides (37%) and the only anthocyanin found (<1%) (Figure 5). Finally, HCA derivatives were less abundant than total flavonoids (Figure 5). The content of diglycosides was generally higher than the content of triglycosides in both wild type and *uvr8-7* plants.

The contents of total HCA derivatives as well as kaempferol and quercetin glycosides containing one rhamnose moiety were consistently higher in the wild type compared to *uvr8-7* plants. Similarly, contents of quercetin glycosides with two rhamnose moieties were higher in the wild type; however, this does not apply to the kaempferol dirhamnose contents, which are the same in both genotypes (Figure 5). Analysis of the contents of several representative individual quercetin glycosides revealed relatively low contents of individual glycosylated quercetins in the *uvr8-7* mutant, compared to the wild type (Figure 6). The quercetin to kaempferol ratio was higher in the wild type than in the *uvr8-7* mutant, reflecting the relatively high level of quercetin glycosides in wild type compared to the *uvr8-7* mutant.

Contents of indole glucosinolates were also higher in the wild type, mainly due to depressed 3-hydroxypropyl glucosinolate and 3-indolylmethylglucosinolate contents in the *uvr8-7* mutant. There were no differences in the overall aliphatic glucosinolate content between the two genotypes (Figure 5).

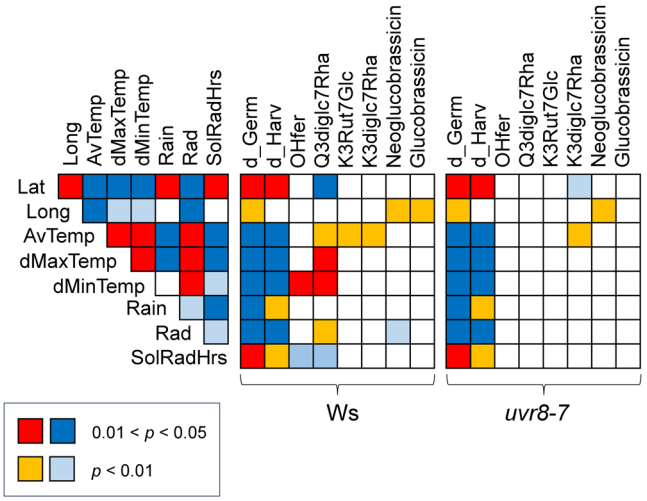


**FIGURE 3** Selected correlations between the geographical, meteorological and physiological variables for two genotypes, *uvr8-7* mutant and the corresponding Wassilewskija (Ws) wild type. Significant ($p < 0.01$ and $0.01 < p < 0.05$) correlations are shown: Positive (red and orange, respectively) and negative (dark and light blue, respectively). AvTemp, average temperature (°C); d_Germ, number of days from sowing to germination; d_Harv, number of days from sowing to harvest (flowering); dMaxTemp, daily maximum temperature (°C); dMinTemp, daily minimum temperature (°C); Glucobrassicin, 3-Indolylmethylglucosinolate; K3diglc7Rha, kaempferol 3-diglucoside 7-rhamnoside; K3Rut7Glc, kaempferol 3-rutinoside 7-glucoside; Lat, latitude (°N); Long, longitude (°E); Neoglucobrassicin, 1-methoxy-3-indolylmethylglucosinolate; OHfer, hydroxy-feruloyl-glucoside; Q3diglc7Rha, quercetin 3-diglucoside 7-rhamnoside; Rad, total radiation (MJ $m^{-2}$ $day^{-1}$). [Color figure can be viewed at wileyonlinelibrary.com]

## 3.4 | Effect of latitude and associated meteorological variables

Regarding both genotypes examined, latitude was positively correlated with the length of the periods from sowing to germination and from sowing to harvest ($p < 0.01$) (Figure 3). Thus, with higher latitude (and correspondingly lower temperature and radiation), the time periods required for germination and flowering were longer. However, latitude and its meteorological covariables average, maximal and minimal temperature and total radiation were not correlated with plant growth variables (rosette size, DW) or with the overall contents of glucosinolates, flavonoid glycosides and HCA derivatives in any genotype (Supporting Information S1: Table S5). However, although no correlations were observed over the period from germination to harvest, it can't be excluded that short-term weather variations modify plant growth variables at specific locations.

In the wild type, several individual compounds (hydroxyferuloyl-glucoside, quercetin 3-diglucoside 7-rhamnoside, and kaempferol 3-rutinoside 7-glucoside) were significantly positively correlated with temperature (either average, maximum and/or minimum) and/or radiation, whereas neoglucobrassicin, a glucosinolate, was negatively correlated with radiation (Figure 3). In particular, quercetin 3-diglucoside 7-rhamnoside was negatively correlated with latitude and positively with AvTemp, dMaxTemp, dMinTemp and Rad. However, no consistent correlation between meteorological variables and metabolites was found in *uvr8-7* (Figure 3 and Supporting Information S1: Table S5).

To study in more detail the effect of latitude on the differences between both genotypes, the differential accumulation of secondary metabolites across both genotypes was analysed as a function of latitude (Figure 7). There was a negative correlation between latitude and content of total flavonoids and total quercetin glycosides in wild type versus *uvr8-7*. Thus, at higher latitudes the difference in total flavonoids and total quercetin glycosides between wild type and uvr8-7

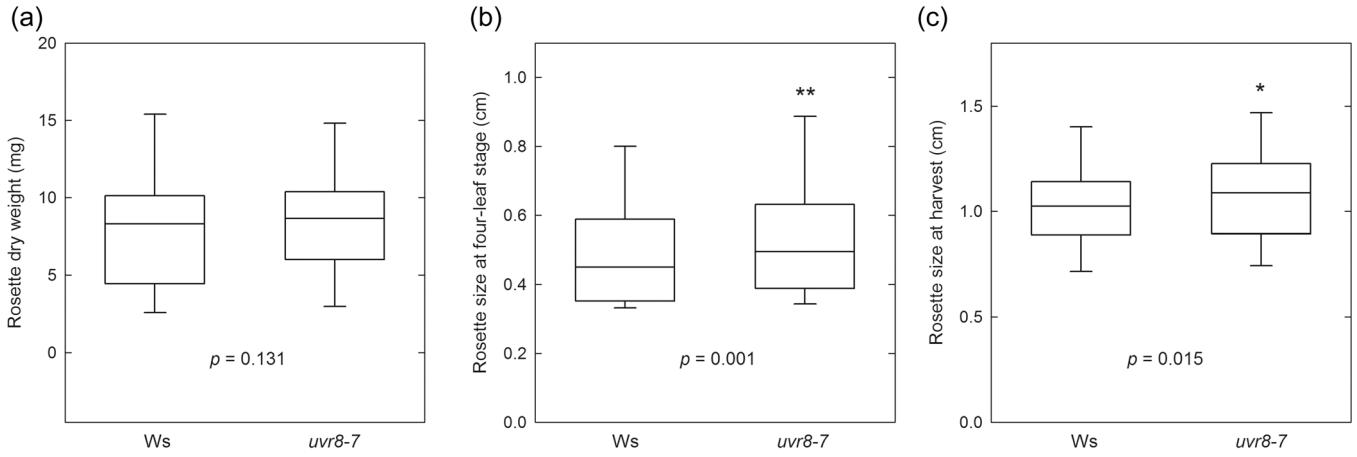


**FIGURE 4** Boxplots of (a) dry weight (DW) per plant at harvest and rosette size at (b) thinning (four-leaf stage) and (c) harvest, in the two *Arabidopsis* genotypes used (Wassilewskija [Ws] wild type and the mutant *uvr8-7*). Box, upper and lower quartiles; line, median; whiskers, 10% and 90% percentiles. The *p* value for Mann–Whitney test is shown to compare groups.

were relatively small. Similarly, the total quercetin to total kaempferol ratio was also latitude dependent, with differences between the two genotypes being relatively large at lower latitudes, and small at higher latitudes. However, there was no correlation between latitude and differential contents of total kaempferol glycosides, total HCA derivatives, and total glucosinolates between the two genotypes. Thus, in more southerly locations (with higher temperatures and radiation) wild-type plants accumulated (1) relatively more total flavonoids and total quercetin glycosides, and (2) had a higher quercetin to kaempferol ratio compared to *uvr8-7* plants.

### 3.5 | Detailed analysis of patterns in the multiparameter data set

Relationships between variables for each of the two genotypes grown at the 21 locations were assessed through two different PCAs. In the first PCA (Figure 8), all the geographic, meteorological and physiological variables were considered. The accumulated variance explained by the first two axes was 56% (34% for axis I and 22% for axis II). In the biplot constructed using these two axes, the locations broadly segregated along Axis I related to latitude and its associated meteorological and developmental variables. Latitude and the periods from sowing to both germination and flowering were significant loading factors for the negative part of Axis I, whereas AvTemp was the most significant loading factor for the positive part of Axis I. Thus, the northerly and colder locations, where plant development was slower, were found towards the negative part of the axis, whereas the more southerly and warmer locations, where plants developed faster, clustered toward the positive part. The only metabolite group acting as a loading factor for axis I was HCA derivatives, indicating a trend for higher HCA contents in plants at southern locations, with lower latitudes and higher AvTemp values (although HCA content was not correlated with latitude or AvTemp, see Figure 7 and Supporting Information S1: Table S5). The two genotypes were hardly differentiated by the first axis, and thus near vertical lines joined the two genotypes at each location.

Regarding Axis II (Figure 8), flavonol glycosides (and the anthocyanin) were the most significant loading factors for its positive part, whereas the three growth variables (the rosette size at both thinning and harvest, together with the DW per plant at harvest) were significant factors for the negative part. Hence, axis II clearly separated the two genotypes for each location, based on the smaller size and higher flavonol glycosides contents of wild-type plants in comparison with *uvr8-7* plants.

In the second PCA (Supporting Information S1: Figure S1), we only used growth variables and the contents of individual metabolites, to test if the ordination of locations and genotypes would remain the same as in the first PCA, once the influences of latitude and its associated meteorological (temperatures and radiation) and developmental variables (periods from sowing to germination and harvest) were excluded. The cumulative variance explained by the first two axes was very similar to that found in the first PCA (35% for Axis I and 22% for Axis II, for a total of 57%). In the plot generated using these two axes, the ordination of the locations was much more blurred than in the first PCA (Figure 8), although the differentiation of the two genotypes remained clear. Most phenolic compounds (quercetin glycosides, kaempferol glycosides, the quercetin and kaempferol ratio, the anthocyanin and some HCA derivatives) were the most significant loading factors for the positive part of Axis I, whereas one HCA derivative (sinapic acid) and the rosette size at harvest were the most significant loading factors for the negative part. Thus, wild type and *uvr8-7* plants were mostly situated towards the positive and negative parts of Axis I, respectively, due to the higher contents of phenolic compounds in wild type than in *uvr8-7* (Figure 5). Regarding Axis II, glucosinolates were significant loading factors for its positive part, whereas there was no clear loading factor for its negative part. Neither locations nor genotypes were clearly separated along Axis II.

## 4 | DISCUSSION

### 4.1 | Unique field study across a wide latitude gradient

Here, a nonsense mutant of the UV-B photoreceptor UVR8 (*uvr8-7*) and its corresponding wild-type accession were used to test the functional importance of UVR8 under field conditions across a latitudinal gradient of 27° (around 3000 km of linear distance). This gradient is even longer (almost double) than previous gradients used to study effects of UV radiation on grapevine (Castagna et al., 2017; Del-Castillo-Alonso et al., 2016) and covers almost the entire area of Europe where natural *Arabidopsis* populations have been found (Beck et al., 2008; Fournier-Level et al., 2011; Hancock et al., 2011; Lee et al., 2017; Alonso-Blanco et al., 2016). This latitudinal gradient encompasses substantial natural variation in meteorological parameters, including temperature, and solar radiation (Supporting Information S1: Table S1). Thus, the experimental setup facilitates the study of UVR8 function in relation to diverse environmental parameters.

The role of UVR8 has rarely been tested under field conditions (Coffey et al., 2017; Findlay & Jenkins, 2016; Stockenhuber et al., 2024) and never across such a wide climatic-latitudinal gradient. This study reveals clear genotypic effects across diverse environments, Thus, the different behaviour of the two genotypes across different environments demonstrated a crucial role of UVR8 in controlling both phenotypic variables (plant size) and secondary plant metabolite composition, notwithstanding that the function of UVR8 is modulated by interactions with other photoreceptor signalling pathways (Huang et al., 2013; Mazza & Ballaré, 2015; Morales et al., 2013; Podolec & Ulm, 2018; Rai et al., 2020). Yet, this study also shows how the functional role of UVR8 is context dependent, with differential effects on metabolites being latitude dependent.

### 4.2 | Genotype-dependent rosette morphology

The longer time periods from sowing to germination and from sowing to flowering are concordant with the slower development

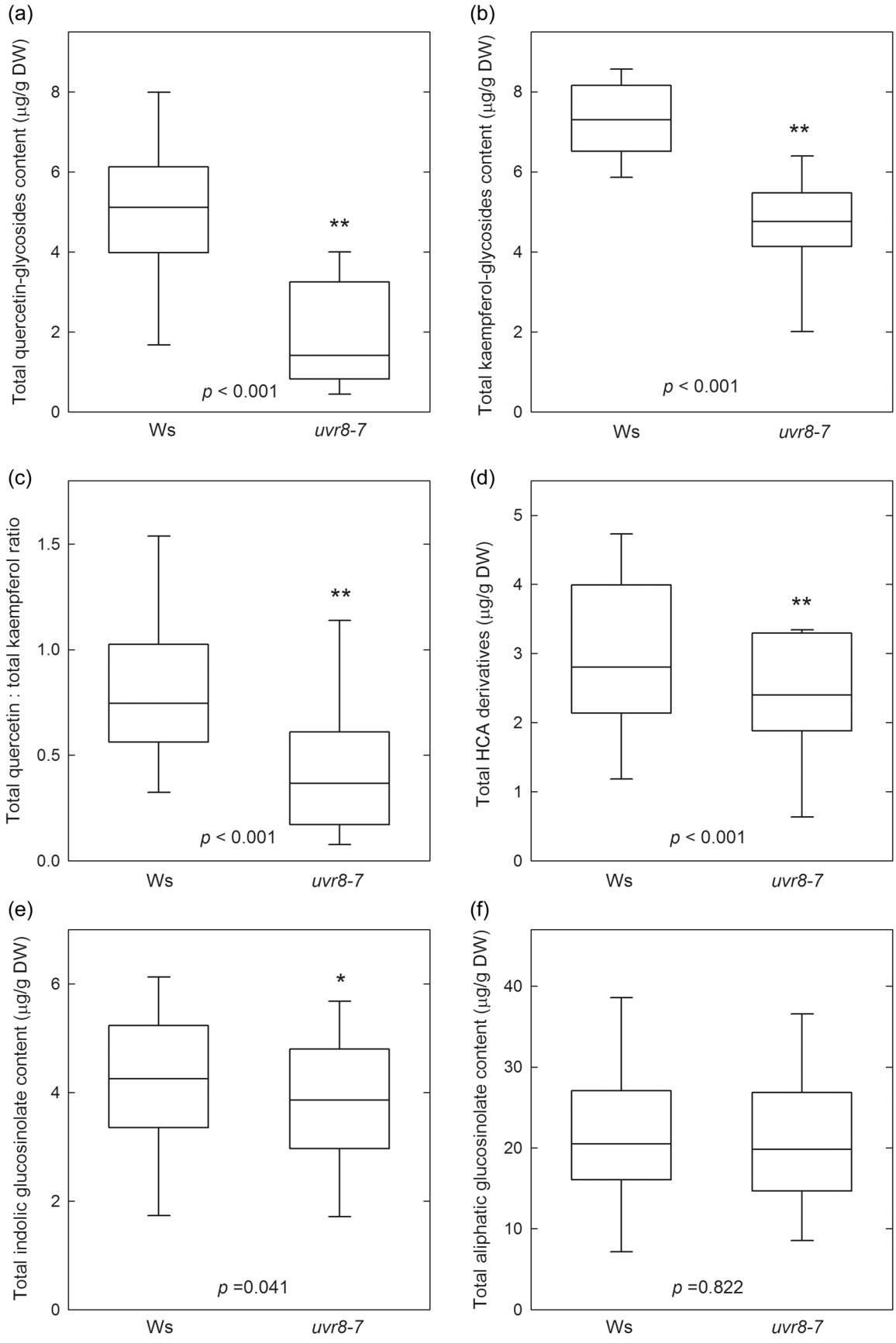


**FIGURE 5** (See caption on next page).

for the *uvr8-7* mutant and the wild-type plants at higher latitudes, corresponding to lower temperature and radiation (Figure 3). However, the results revealed that the *uvr8-7* mutant was not only able to grow under natural, solar conditions, despite lack the UVR8 photoreceptor, but it also produced larger rosettes than the wild type (Figure 4 and Supporting Information S1: Table S3). This occurred irrespective of latitude, temperature, and radiation conditions, as shown by (1) the lack of correlations between geographic-environmental variables and plant biomass and morphology (Figure 3 and Supporting Information S1: Table S5); and (2) the similar distances between both genotypes in the PCA performed (Figure 8), irrespective of latitude and associated climatic variables.

A 'dwarfing' effect of an activated functional UV-B regulatory pathway on morphology is commonly reported in laboratory studies (Robson et al., 2015). Here, it is revealed that such a response is also found in complex, outdoor environments, such as in the present study (i.e. the wild type is here smaller under ambient UV-B exposure than *uvr8-7*). This outcome is particularly interesting since many other environmental factors, such as light quality (Sommer et al., 2023), high salinity (Navarro et al., 2007), low temperature (Rodríguez et al., 2015) and drought (Rodríguez-Calzada et al., 2019), are all

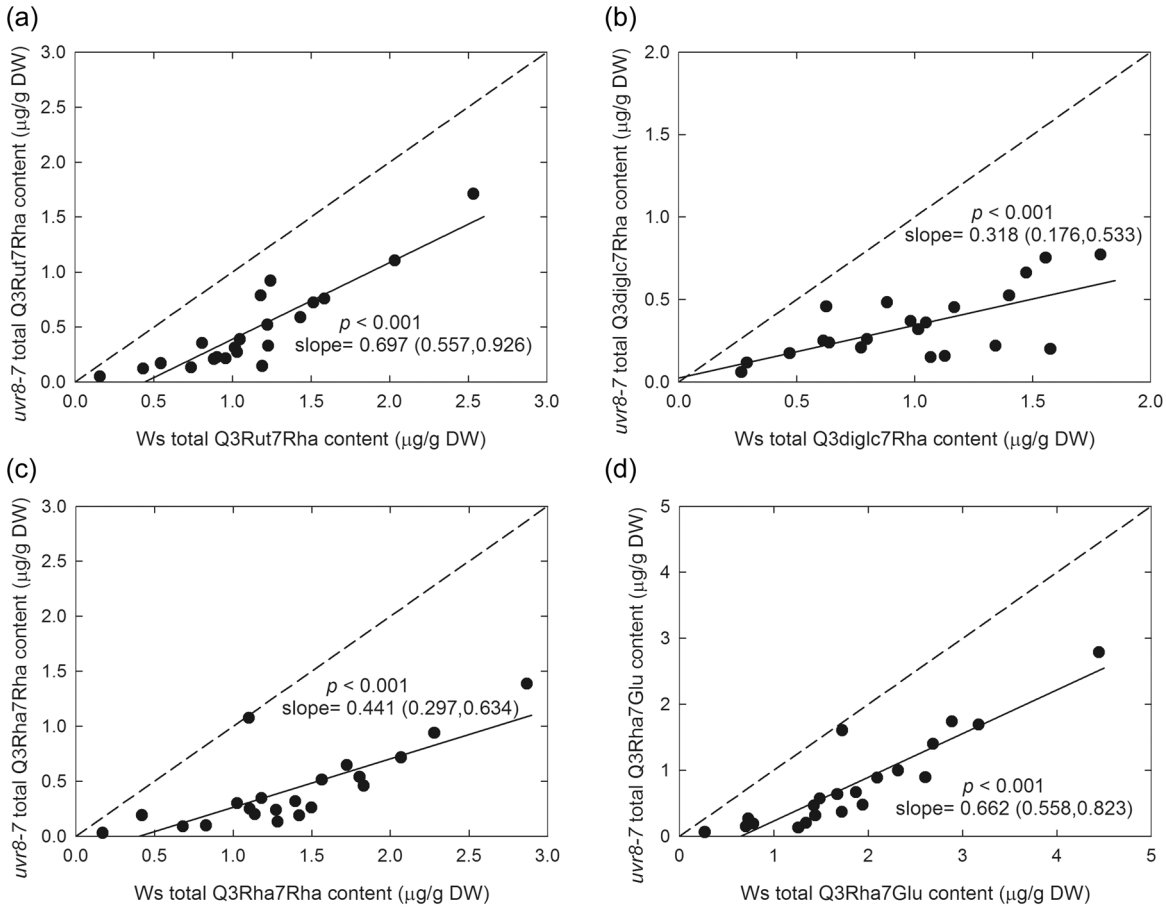


**FIGURE 6** Correlations between metabolite contents of the two Arabidopsis genotypes (Wassilewskija [Ws] wild type and mutant *uvr8-7*). (a) Q3Rut7Rha, quercetin 3-rutinoside 7-rhamnoside; (b) Q3diglc7Rha, quercetin 3-diglucoside 7-rhamnoside; (c) Q3Rha7Rha, quercetin 3-rhamnoside 7-rhamnoside; (d) Q3Rha7Glu, quercetin 3-rhamnoside 7-glucoside. For each compound, an *x*–*y* plot is shown using mean contents measured in wild type and *uvr8-7* plants as *x* and *y* coordinates, respectively. Different dots correspond to different locations, and their position relative to the *x* = *y* dashed line indicates whether mean contents differed between the two genotypes (dot on the line) or were higher in wild type than in *uvr8-7* plants (dot under the dashed line). Linear fits of the wild type–*uvr8-7* data pairs are shown as a solid line, with their respective slopes and confidence intervals of the model fit, and *p* values ($n = 21$).

**FIGURE 5** Boxplots of the different classes of plant secondary metabolites analysed at harvest in the two *Arabidopsis* genotypes used (Wassilewskija [Ws] wild type and the mutant *uvr8-7*): (a) total quercetin glycosides, (b) total kaempferol glycosides, (c) quercetin to kaempferol ratio, (d) total hydroxycinnamic acid (HCA) derivatives, (e) total indolic glucosinolates and (f) total aliphatic glucosinolates. Box, upper and lower quartiles; line, median; whiskers, 10% and 90% percentiles. The *p* value for Mann–Whitney test is shown to compare groups.

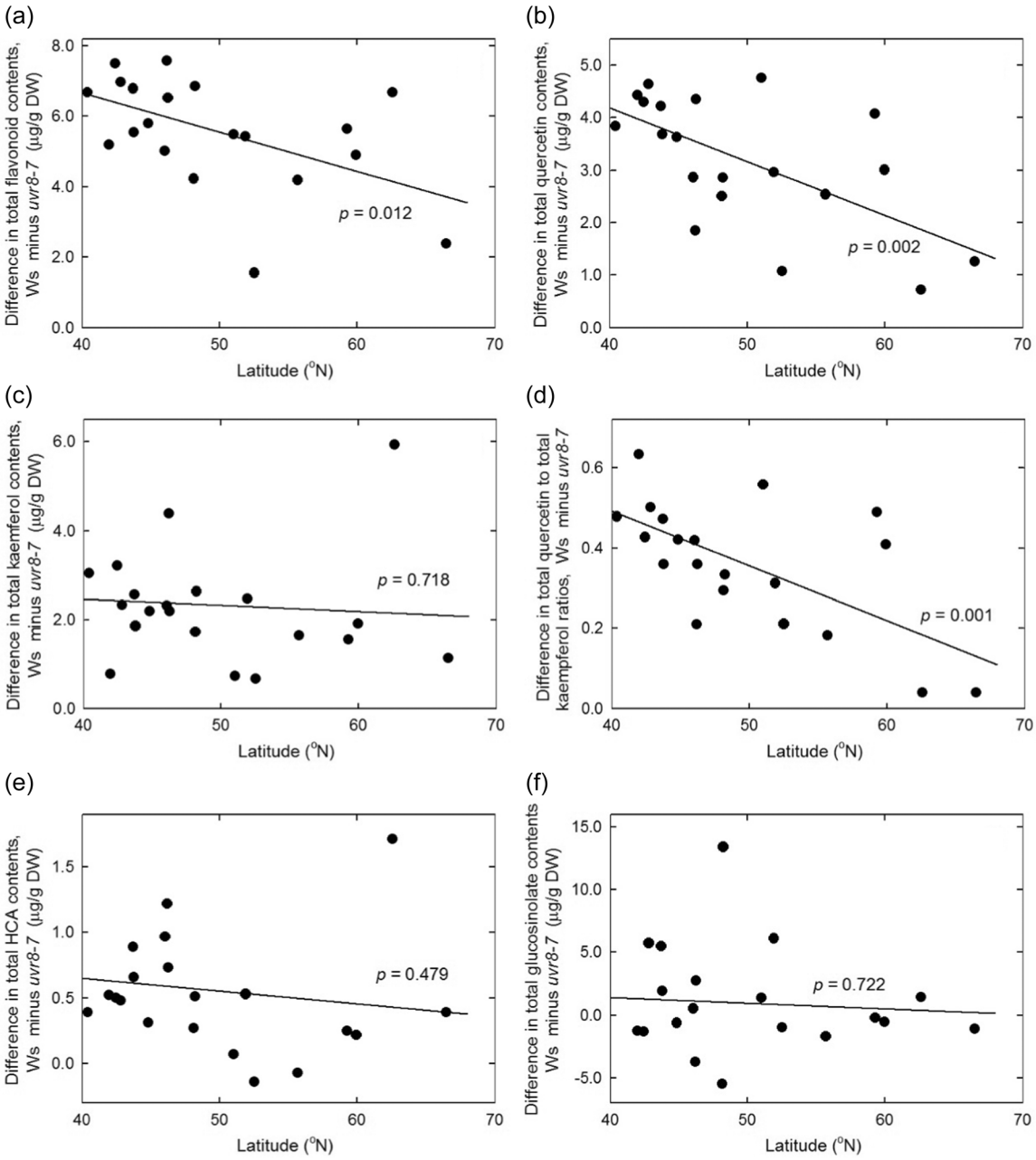


**FIGURE 7** The effect of latitude on the differential accumulation of metabolites (a), total flavonoids; (b), total quercetin glycosides; (c), total kaempferol glycosides; (d), the quercetin to kaempferol ratio; (e), total hydroxycinnamic acid (HCA) derivatives; and (f), total glucosinolates) in the two *Arabidopsis* genotypes (Wassilewskija [Ws] wild type and mutant *uvr8-7*). The probability that a difference between the two genotypes is linearly dependent on latitude is shown (*p* value).

known to alter plant morphology in a similar fashion but despite this did not mask this UV response. Thus, the data in this study reveal the relative importance of UV-B radiation and its perception in inducing morphological changes across a wide range of environments. In this context, the 'dwarfing' effect could be interpreted as an indirect trade-off 'cost', in the form of altered growth parameters associated with activity of the UVR8-dependent regulatory pathway. Conversely, it could be argued that 'dwarfing' directly contributes to protection from UV-radiation stress, or even has a more-indirect role in protecting against other environmental factors such as drought (Jansen et al., 2022).

UV radiation increases with decreasing latitude (Aphalo et al., 2012). However, the data in this study do not show a parallel, latitude dependent increase in morphological 'dwarfing' of the plants. Thus, 'dwarfing' is dependent on UVR8 but not on latitude. It is argued that the overall effect of UV radiation on plant morphology is qualitative rather than quantitative, depending on the UVR8 photoreceptor, but not on the UV-B dose received by the plant.

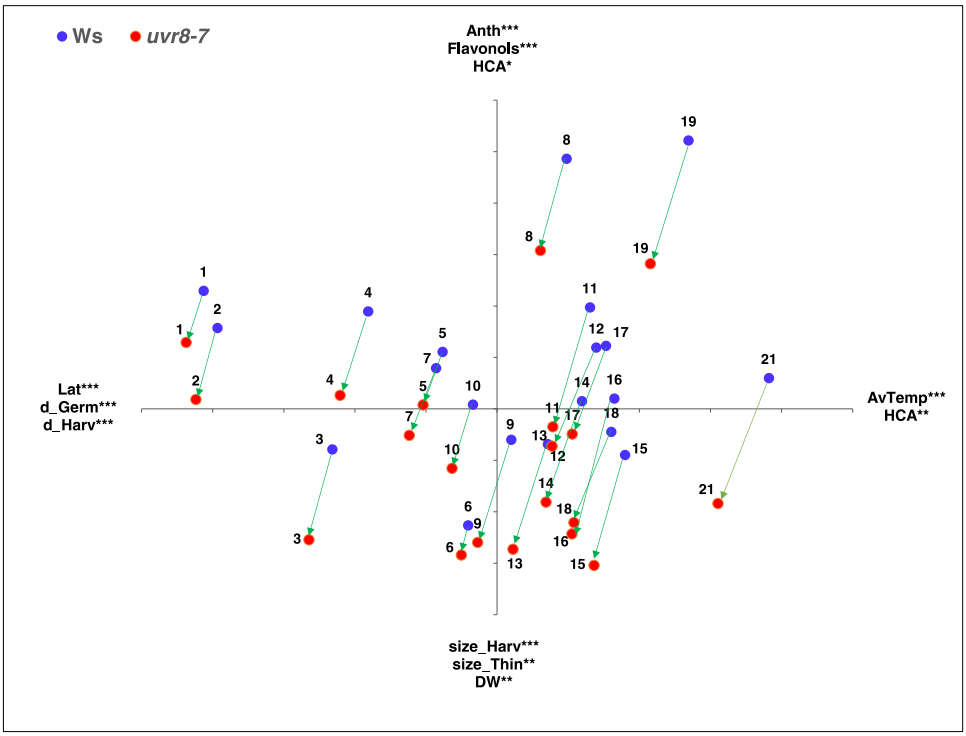


**FIGURE 8** Ordination, through principal components analysis (PCA), of the two genotypes (Wassilewskija [Ws] wild type, blue dots, and mutant *uvr8-7*, red dots) at the 21 locations of the present study, using geographic, meteorological and physiological variables. The two genotypes for each location are joined by arrows to show their relative places. The significant loading factors for the positive and negative parts of each axis, together with their corresponding significance levels, are shown (***$p < 0.001$; **$p < 0.01$; *$p < 0.05$). The accumulated variance by Axes I and II was 34% and 22%, respectively. Each tick mark on axes I and II represents 0.5 units. Anth, anthocyanin; AvTemp, average temperature in the period from sowing to harvest; d_Germ, days from sowing to germination; d_Harv, days from sowing to harvest (flowering); DW, dry weight per plant at harvest; HCA, hydroxycinnamic acid derivatives; Lat, latitude; size_Thin and size_Harv, rosette size at thinning (four-leaf stage) and harvest, respectively. [Color figure can be viewed at wileyonlinelibrary.com]

## 4.3 | Genotype-dependent changes in secondary plant metabolite profiles

The contents of all flavonoids and HCA derivatives were higher in wild type than in *uvr8-7*. Flavonoids and HCA derivatives are groups of compounds that are frequently enhanced by UV radiation and implicated in protection against UV exposure. Hence, the results confirm that the UVR8 photoreceptor plays a key role in regulating accumulation of flavonoids and HCA derivatives, even under variable environmental conditions that, as potential promoters of phenolic biosynthesis themselves (Cheynier et al., 2013), could mask, or even overwhelm, UV effects at the scale typically found under controlled laboratory conditions.

The higher quercetin to kaempferol ratio in the wild type compared to *uvr8-7* comprises a quantitative effect that links the presence of functional UVR8 to specific changes in the flavonoid profile. Polyhydroxylated quercetin glycosides have higher antioxidant activity compared to monohydroxylated kaempferol glycosides (Majer et al., 2014) and, therefore, the accumulation of quercetin glycosides has been linked to stress-resistance. The synthesis of quercetin from kaempferol requires a flavonoid hydroxylation step, which is usually performed by a cytochrome P450 flavonoid monooxygenase, associated to a cytochrome P450 reductase, and utilizing $O_2$ and NADPH (Leonard et al., 2006). Furthermore, UVR8, via Myb12, induces expression of flavonol synthase to a greater extent than that of flavonol 3′-hydroxylase, responsible for the conversion of kaempferol into quercetin (Mehrtens et al., 2005). This may lead to a lower proportion of hydroxylated flavonols (Martínez-Lüscher et al., 2014). The results presented here demonstrate the importance of UVR8 in mediating this conversion from kaempferol to quercetin under widely different environmental conditions. Furthermore, there are certain quercetin glycosides that only accumulate in wild type plants and not *uvr8-7*: here, the wild type was particularly enriched in quercetin 3-rhamnoside 7-rhamnoside and quercetin 3-diglucoside 7-rhamnoside. Likewise, indoor experiments also found UV-induced increases in quercetin 3-rhamnoside 7-rhamnoside as well as quercetin 3-diglucoside 7-rhamnoside (as well as some kaempferol glycosides) in Arabidopsis (Neugart et al., 2019). Taken together, this may imply that expression of the flavonol 7-O-rhamnosyltransferase encoding gene UGT89C1 is UVR8-dependent (Hectors et al., 2014), which would mean that the UV-B photoreceptor controls multiple aspects of flavonoid biosynthesis.

### 4.4 | Latitude dependent changes in metabolite profiles

Differences in metabolite contents between genotypes were latitude dependent for total flavonoids, quercetin glycosides and the quercetin-to-kaempferol ratio. Wild-type plants accumulated relatively more total flavonoids and quercetin glycosides than *uvr8-7* plants in more southerly locations (with higher temperatures, higher global and UV radiation). Compared to *uvr8-7* plants, wild-type plants also accumulated relatively more quercetin glycosides than kaempferol glycosides, at more southerly locations. Hence, the lower the latitude, the larger the impact of UVR8. At present, it remains to be seen whether the variable size of the response represents a quantitative UVR8 photoreceptor response, or rather interactive, downstream effects of UVR8 and other environmental factors such as temperature and global radiation. Earlier studies reported that the accumulation of UVR8 monomers, required for active UVR8-mediated signalling, is temperature dependent (Findlay & Jenkins, 2016). Furthermore, accumulation of specific metabolites also showed a strong correlation with temperature (Figure 3 and Supporting Information S1: Table S5), an observation that is consistent with the published literature. For example, Coffey and Jansen (2019), and Pescheck and Bilger (2019) showed significant effects of temperature on quercetin accumulation in outdoor experiments. Thus, temperature is a possible environmental factor that can modulate the extent of UV responses.

Kaempferol glycoside contents were not affected by latitude, although quercetin glycoside contents are (Figure 7). Kaempferol is a precursor to the biosynthesis of quercetin and it is possible that plants accumulate a pool of kaempferol, which is only converted to quercetin when required, for example during UV exposure. This suggestion is in agreement with quercetin being both a better antioxidant (Majer et al., 2014) and a better peroxidase substrate (Yamasaki et al., 1997) than kaempferol.

Just one indole glucosinolate, neoglucobrassicin, displayed a slight negative radiation-associated response. UV-B-driven glucosinolate speciation is known to rely on functional PDX (pyridoxine, vitamin B6) (Neugart et al., 2020), a step which potentially uncouples glucosinolate content from UVR8 activity. Furthermore, some classes of glucosinolates (e.g., aliphatic glucosinolates) are less responsive to environmental factors than others (e.g., indole glucosinolates) (Bohinc & Trdan, 2012). Consistently, it was found that overall, glucosinolate contents did not differ substantially between genotypes, and as a function of geographic-environmental variables. Their relatively constitutive expression is consistent with a predominant role as deterrent against herbivores and pathogens, rather than in UV protection.

## 5 | CONCLUSION

This study revealed the functional role of the plant UV-B photoreceptor, UVR8 using a large-scale synchronized genetic-perturbation field experiment. Under realistic, and highly varied, field conditions, it was found that the *uvr8* mutation had a strong impact on morphology and contents of hydroxycinnamic acid derivatives, glycosylated quercetins and kaempferols, as well as the quercetin to kaempferol ratio, in *Arabidopsis*. Thus, the functional importance of the UVR8 photoreceptor is notable under varied, natural environmental conditions notwithstanding the presence of other environmental signalling pathways that might have otherwise been expected to mask UVR8 effects.

The quantitative effect of functional UVR8 on contents of total flavonoids, total quercetin glycosides and the quercetin-to-kaempferol ratio is variable and increased with decreasing latitude. At present it remains to be seen whether the variable effect is causally linked to a corresponding quantitative UVR8 response, or rather whether interactive effects of UVR8 and other environmental factors such as temperature and global radiation modulate UV responses. Conversely, UVR8-mediated effects on morphology and kaempferol glycoside contents were similar across a large latitudinal-climatic gradient, suggesting that these effects are qualitative; that is, the effect does not depend on the UV-B doses but only on the presence of the photoreceptor. It appears that under field conditions both of these UVR8-mediated effects are evident in the phenotype. Thus, this study not only reveals a functional role for the UVR8 photoreceptor under natural conditions, but it also indicates, thus far, unknown levels of regulatory control.


### AFFILIATIONS

[1]Division Quality and Sensory of Plant Products, Georg-August-Universität Göttingen, Göttingen, Germany

[2]Department of Applied Genetics & Cell Biology, University of Natural Resources & Life Sciences, Vienna, Austria

[3]Faculty of Science and Technology, University of La Rioja, Logrono, Spain

[4]Leibniz Institute of Vegetable and Ornamental Crops, Großbeeren, Germany

[5]Department of Natural Sciences, School of Science and Technology, Örebro University, Örebro, Sweden

[6]Institute of Plant Biology, HUN-REN Biological Research Centre, Szeged, Hungary

[7]Research Unit Environmental Simulation, Helmholtz Zentrum München, Neuherberg, Germany

[8]Institute of Agricultural Sciences, Spanish Council for Scientific Research, Madrid, Spain

[9]Department of Agriculture, Food and Environment, University of Pisa, Pisa, Italy

[10]Department of Agricultural Production, ETSIAAB, Universidad Politécnica de Madrid, Madrid, Spain

[11]Department of Biology, University of Ljubljana, Ljubljana, Slovenia

[12]Department of Climatology and Landscape Ecology, University of Szeged, Szeged, Hungary

[13]Department of Life Sciences, Aberystwyth University, Aberystwyth, UK

[14]Earthwatch Europe, Oxford, UK

[15]Scion, New Zealand Forest Research Institute, Rotorua, New Zealand

[16]University of Eastern Finland, Joensuu, Finland

[17]Finnish Meteorological Institute – Space and Earth Observation Centre, Sodankylä, Finland

[18]Department of Environmental Sciences, University of Girona, Girona, Spain

[19]Plant Stress Physiology group (Associated Unit to EEAD, CSIC), BIOMA Institute for Biodiversity and the Environment, University of Navarra, Pamplona, Spain

[20]Faculty of Environmental Sciences and Natural Resource Management, Norwegian University of Life Sciences, Ås, Norway

[21]Department of Plant Sciences, Norwegian University of Life Sciences, Ås, Norway

[22]Earth and Environment Sciences, Forel Institute, Geneva University, Geneva, Switzerland

[23]Organismal & Evolutionary Biology (OEB), Viikki Plant Science Centre (ViPS), Faculty of Biological & Environmental Sciences, University of Helsinki, Helsinki, Finland

[24]National School of Forestry, University of Cumbria, Ambleside, UK

[25]Institute of Plant and Environmental Sciences, Crop Science, University of Copenhagen, Tåstrup, Denmark

[26]Arctic Centre, University of Lapland, Rovaniemi, Finland

[27]Department of Physiology, Ghent University, Ghent, Belgium

[28]National Research Council, Institute of Bioeconomy, Sesto Fiorentino, Italy

[29]Laboratory of Monitoring and Environmental Modelling for the Sustainable Development (LaMMA Consortium), Sesto Fiorentino, Italy

[30]National Research Council Institute for Biometeorology, Sesto Fiorentino, Italy

[31]Department of Plant Biology, Faculty of Sciences, University of Pécs, Pécs, Hungary

[32]Environmental Research Institute, School of Biological, Earth, and Environmental Sciences, University College Cork, Cork, Ireland

## ACKNOWLEDGEMENTS

The authors thank Marlies Dolezal for initial statistical support. The following authors gratefully acknowledge financial support: Alenka Gaberscik: Ministry of Higher Education, Science and Innovation, Republic of Slovenia (programme "Biology of plants" P1-0212); Åke Strid: The Carl Trygger Foundation for Scientific Research, Sweden (grant #CTS21:1666), the Knowledge Foundation, Sweden (grant #20130164), the Swedish Research Council Formas, Sweden (grants #942–2015–516) and the Faculty for Business, Science and Technology at Örebro University; András Viczián: the Hungarian Scientific Research Fund (OTKA, K-138022 and K-132633); Beatriz Dáder and Alberto Ferreres: State Investigation Agency, Spain (projects AGL2010-22196-C02-01 and FPI BES-2011-045885); Dolors Verdaguer and Laura Llorens: Spanish Government (project CGL2014-55976-R); Javier Martínez-Abaigar and Encarnación Núñez-Olivera: the Government of La Rioja (project "Afianza" 2023/05); Marcel A. K. Jansen: Science Foundation Ireland (grant number 16-IA-4418); Marie-Theres Hauser: the Austrian Science Fund (FWF) (project F3707); Riitta Julkunen-Tiitto: Academy of Finland (project 267360). The European UV community was supported through COST action FA0906 (UV4growth).

## DATA AVAILABILITY STATEMENT

The data that support the findings of this study are available from the corresponding author upon reasonable request.

## ORCID

*Javier Martínez-Abaigar* http://orcid.org/0000-0002-9762-9862
*Åke Strid* http://orcid.org/0000-0003-3315-8835
*Dylan Gwynn-Jones* http://orcid.org/0000-0002-0645-7584
*Alan Jones* http://orcid.org/0000-0003-3047-3338
*Matthew Robson* https://orcid.org/0000-0002-8631-796X
*Barbro Winkler* http://orcid.org/0000-0002-7092-9742
*Katja Witzel* http://orcid.org/0000-0002-9452-2664
*Daniele Grifoni* http://orcid.org/0000-0002-0811-1624
*Éva Hideg* http://orcid.org/0000-0002-1486-4278
*Marcel A. K. Jansen* http://orcid.org/0000-0003-2014-5859

## REFERENCES

Agati, G. & Tattini, M. (2010) Multiple functional roles of flavonoids in photoprotection. *New Phytologist*, 186, 786–793. Available from: https://doi.org/10.1111/j.1469-8137.2010.03269.x

Alonso-Blanco, C., Andrade, J., Becker, C., Bemm, F., Bergelson, J., Borgwardt, K.M. et al. (2016) 1,135 Genomes reveal the global pattern of polymorphism in *Arabidopsis thaliana*. *Cell*, 166, 481–491. Available from: https://doi.org/10.1016/j.cell.2016.05.063

Aphalo, P.J., Albert, A., Björn, L.O., McLeod, A., Robson, T.M. & Rosenqvist, E. (2012) *Beyond the visible: a handbook of best practice in plant UV photobiology*. University of Helsinki, Department of Biosciences, Division of Plant Biology. Available from: https://doi.org/10.31885/9789521083631

Arongaus, A.B., Chen, S., Pireyre, M., Glöckner, N., Galvão, V.C., Albert, A. et al. (2018) *Arabidopsis* RUP2 represses UVR8-mediated flowering in noninductive photoperiods. *Genes & Development*, 32, 1332–1343. Available from: https://doi.org/10.1101/gad.318592.118

Barnes, P.W., Flint, S.D., Ryel, R.J., Tobler, M.A., Barkley, A.E. & Wargent, J.J. (2015) Rediscovering leaf optical properties: new insights into plant acclimation to solar UV radiation. *Plant Physiology and Biochemistry*, 93, 94–100. Available from: https://doi.org/10.1016/j.plaphy.2014.11.015

Barnes, P.W., Tobler, M.A., Keefover-Ring, K., Flint, S.D., Barkley, A.E., Ryel, R.J. et al. (2016) Rapid modulation of ultraviolet shielding in plants is influenced by solar ultraviolet radiation and linked to alterations in flavonoids. *Plant, Cell & Environment*, 39, 222–230. Available from: https://doi.org/10.1111/pce.12609

Beck, J.B., Schmuths, H. & Schaal, B.A. (2008) Native range genetic variation in *Arabidopsis thaliana* is strongly geographically structured and reflects Pleistocene glacial dynamics. *Molecular Ecology*, 17, 902–915. Available from: https://doi.org/10.1111/j.1365-294X.2007.03615.x

Bernula, P., Crocco, C.D., Arongaus, A.B., Ulm, R., Nagy, F. & Viczián, A. (2017) Expression of the UVR8 photoreceptor in different tissues reveals tissue-autonomous features of UV-B signalling. *Plant, Cell & Environment*, 40, 1104–1114. Available from: https://doi.org/10.1111/pce.12904

Besteiro, M.A.G., Bartels, S., Albert, A. & Ulm, R. (2011) *Arabidopsis* MAP kinase phosphatase 1 and its target MAP kinases 3 and 6 antagonistically determine UV-B stress tolerance, independent of the UVR8 photoreceptor pathway. *The Plant Journal*, 68, 727–737. Available from: https://doi.org/10.1111/j.1365-313X.2011.04725.x

Bohinc, T. & Trdan, S. (2012) Environmental factors affecting the glucosinolate content in Brassicaceae. *J. Food Agric. Environ.* 10, 357–360.

Brown, B.A., Cloix, C., Jiang, G.H., Kaiserli, E., Herzyk, P., Kliebenstein, D.J. et al. (2005) A UV-B-specific signaling component orchestrates plant UV protection. *Proceedings of the National Academy of Sciences*, 102, 18225–18230. Available from: https://doi.org/10.1073/pnas.0507187102

Brown, B.A. & Jenkins, G.I. (2008) UV-B signaling pathways with different fluence-rate response profiles are distinguished in mature *Arabidopsis* leaf tissue by requirement for UVR8, HY5, and HYH. *Plant Physiology*, 146, 323–324. Available from: https://doi.org/10.1104/pp.107.108456

Brown, P.D., Tokuhisa, J.G., Reichelt, M. & Gershenzon, J. (2003) Variation of glucosinolate accumulation among different organs and

developmental stages of *Arabidopsis thaliana*. *Phytochemistry*, 62, 471–481. Available from: https://doi.org/10.1016/s0031-9422(02)00549-6

Castagna, A., Csepregi, K., Neugart, S., Zipoli, G., Večeřová, K., Jakab, G. et al. (2017) Environmental plasticity of pinot noir grapevine leaves: a trans-European study of morphological and biochemical changes along a 1,500-km latitudinal climatic gradient. *Plant, Cell & Environment*, 40, 2790–2805. Available from: https://doi.org/10.1111/pce.13054

Chen, M., Chory, J. & Fankhauser, C. (2004) Light signal transduction in higher plants. *Annual Review of Genetics*, 38, 87–117. Available from: https://doi.org/10.1146/annurev.genet.38.072902.092259

Cheynier, V., Comte, G., Davies, K.M., Lattanzio, V. & Martens, S. (2013) Plant phenolics: recent advances on their biosynthesis, genetics, and ecophysiology. *Plant Physiology and Biochemistry*, 72, 1–20. Available from: https://doi.org/10.1016/j.plaphy.2013.05.009

Chory, J. (2010) Light signal transduction: an infinite spectrum of possibilities. *The Plant Journal*, 61, 982–991. Available from: https://doi.org/10.1111/j.1365-313X.2009.04105.x

Coffey, A. & Jansen, M.A.K. (2019) Effects of natural solar UV-B radiation on three *Arabidopsis* accessions are strongly affected by seasonal weather conditions. *Plant Physiology and Biochemistry*, 134, 64–72. Available from: https://doi.org/10.1016/j.plaphy.2018.06.016

Coffey, A., Prinsen, E., Jansen, M.A.K. & Conway, J. (2017) The UVB photoreceptor UVR8 mediates accumulation of UV-absorbing pigments, but not changes in plant morphology, under outdoor conditions. *Plant, Cell & Environment*, 40, 2250–2260. Available from: https://doi.org/10.1111/pce.13025

Del-Castillo-Alonso, M.Á., Castagna, A., Csepregi, K., Hideg, É., Jakab, G., Jansen, M.A.K. et al. (2016) Environmental factors correlated with the metabolite profile of *Vitis vinifera* cv. pinot noir berry skins along a European latitudinal gradient. *Journal of Agricultural and Food Chemistry*, 64, 8722–8734. Available from: https://doi.org/10.1021/acs.jafc.6b03272

Demkura, P.V. & Ballaré, C.L. (2012) UVR8 mediates UV-B-induced *Arabidopsis* defense responses against *Botrytis cinerea* by controlling sinapate accumulation. *Molecular Plant*, 5, 642–652. Available from: https://doi.org/10.1093/mp/sss025

Favory, J.-J., Stec, A., Gruber, H., Rizzini, L., Oravecz, A., Funk, M. et al. (2009) Interaction of COP1 and UVR8 regulates UV-B-induced photomorphogenesis and stress acclimation in *Arabidopsis*. *The EMBO Journal*, 28, 591–601. Available from: https://doi.org/10.1038/emboj.2009.4

Fernández, M.B., Tossi, V., Lamattina, L. & Cassia, R. (2016) A comprehensive phylogeny reveals functional conservation of the UV-B photoreceptor UVR8 from green algae to higher plants. *Frontiers in Plant Science*, 7, 1698. Available from: https://doi.org/10.3389/fpls.2016.01698

Findlay, K.M.W. & Jenkins, G.I. (2016) Regulation of UVR8 photoreceptor dimer/monomer photo-equilibrium in *Arabidopsis* plants grown under photoperiodic conditions. *Plant, Cell & Environment*, 39, 1706–1714. Available from: https://doi.org/10.1111/pce.12724

Fournier-Level, A., Korte, A., Cooper, M.D., Nordborg, M., Schmitt, J. & Wilczek, A.M. (2011) A map of local adaptation in *Arabidopsis thaliana*. *Science*, 334, 86–89. Available from: https://doi.org/10.1126/science.1209271

Hammer, Ø., Harper, D.A.T. & Ryan, P.D. (2001) PAST: Paleontological Statistics Software Package for education and data analysis. *Palaeontologia Electronica*, 4, 9.

Hancock, A.M., Brachi, B., Faure, N., Horton, M.W., Jarymowycz, L.B., Sperone, F.G. et al. (2011) Adaptation to climate across the *Arabidopsis thaliana* genome. *Science*, 334, 83–86. Available from: https://doi.org/10.1126/science.1209244

Hauser, M.T., Adhami, F., Dorner, M., Fuchs, E. & Glössl, J. (1998) Generation of co-dominant PCR-based markers by duplex analysis on high resolution gels. *The Plant Journal*, 16, 117–125. Available from: https://doi.org/10.1046/j.1365-313x.1998.00271.x

Hectors, K., Van Oevelen, S., Geuns, J., Guisez, Y., Jansen, M.A.K. & Prinsen, E. (2014) Dynamic changes in plant secondary metabolites during UV acclimation in *Arabidopsis thaliana*. *Physiologia Plantarum*, 152, 219–230. Available from: https://doi.org/10.1111/ppl.12168

Hectors, K., Prinsen, E., De Coen, W., Jansen, M.A.K. & Guisez, Y. (2007) *Arabidopsis thaliana* plants acclimated to low dose rates of ultraviolet B radiation show specific changes in morphology and gene expression in the absence of stress symptoms. *New Phytologist*, 175, 255–270. Available from: https://doi.org/10.1111/j.1469-8137.2007.02092.x

Huang, X., Ouyang, X., Yang, P., Lau, O.S., Chen, L., Wei, N. et al. (2013) Conversion from CUL4-based COP1-SPA E3 apparatus to UVR8-COP1-SPA complexes underlies a distinct biochemical function of COP1 under UV-B. *Proceedings of the National Academy of Sciences*, 110, 16669–16674. Available from: https://doi.org/10.1073/pnas.1316622110

Ibdah, M., Krins, A., Seidlitz, H.K., Heller, W., Strack, D. & Vogt, T. (2002) Spectral dependence of flavonol and betacyanin accumulation in *Mesembryanthemum crystallinum* under enhanced ultraviolet radiation. *Plant, Cell & Environment*, 25, 1145–1154. Available from: https://doi.org/10.1046/j.1365-3040.2002.00895.x

Jansen, M.A.K., Ač, A., Klem, K. & Urban, O. (2022) A meta-analysis of the interactive effects of UV and drought on plants. *Plant, Cell & Environment*, 45, 41–54. Available from: https://doi.org/10.1111/pce.14221

Jansen, M.A.K., Bilger, W., Hideg, É., Strid, Å., Urban, O., Aphalo, P. et al. (2019) Editorial: interactive effects of UV-B radiation in a complex environment. *Plant Physiology and Biochemistry*, 134, 1–8. Available from: https://doi.org/10.1016/j.plaphy.2018.10.021

Jenkins, G.I. (2009) Signal transduction in responses to UV-B radiation. *Annual Review of Plant Biology*, 60, 407–431. Available from: https://doi.org/10.1146/annurev.arplant.59.032607.092953

Kami, C., Lorrain, S., Hornitschek, P. & Fankhauser, C. (2010) Light-regulated plant growth and development. *Current Topics in Developmental Biology*, 91, 29–66. Available from: https://doi.org/10.1016/S0070-2153(10)91002-8

Kliebenstein, D.J., Lim, J.E., Landry, L.G. & Last, R.L. (2002) Arabidopsis UVR8 regulates ultraviolet-b signal transduction and tolerance and contains sequence similarity to human regulator of chromatin condensation 1. *Plant Physiology*, 130, 234–243. Available from: https://doi.org/10.1104/pp.005041

Krumbein, A., Schonhof, I. & Schreiner, M. (2005) Composition and contents of phytochemicals (glucosinolates, carotenoids and chlorophylls) and ascorbic acid in selected *Brassica* species (*B. juncea*, *B. rapa* subsp. nipposinica var. chinoleifera, *B. rapa* subsp. chinensis and *B. rapa* subsp. rapa). *J. Appl. Bot. Food Qual.* 79, 168–174.

Kusano, M., Tohge, T., Fukushima, A., Kobayashi, M., Hayashi, N., Otsuki, H. et al. (2011) Metabolomics reveals comprehensive reprogramming involving two independent metabolic responses of *Arabidopsis* to UV-B light. *The Plant Journal*, 67, 354–369. Available from: https://doi.org/10.1111/j.1365-313X.2011.04599.x

Leonard, E., Yan, Y. & Koffas, M. (2006) Functional expression of a P450 flavonoid hydroxylase for the biosynthesis of plant-specific hydroxylated flavonols in *Escherichia coli*. *Metabolic Engineering*, 8, 172–181. Available from: https://doi.org/10.1016/j.ymben.2005.11.001

Lee, C.-R., Svardal, H., Farlow, A., Exposito-Alonso, M., Ding, W., Novikova, P. et al. (2017) On the post-glacial spread of human commensal *Arabidopsis thaliana*. *Nature Communications*, 8, 14458. Available from: https://doi.org/10.1038/ncomms14458

Majer, P., Neugart, S., Krumbein, A., Schreiner, M. & Hideg, É. (2014) Singlet oxygen scavenging by leaf flavonoids contributes to sunlight acclimation in *Tilia platyphyllos*. *Environmental and Experimental Botany*, 100, 1–9. Available from: https://doi.org/10.1016/j.envexpbot.2013.12.001

Martínez-Lüscher, J., Torres, N., Hilbert, G., Richard, T., Sánchez-Díaz, M., Delrot, S. et al. (2014) Ultraviolet-B radiation modifies the quantitative and qualitative profile of flavonoids and amino acids in grape berries. *Phytochemistry*, 102, 106–114. Available from: https://doi.org/10.1016/j.phytochem.2014.03.014

Mazza, C.A. & Ballaré, C.L. (2015) Photoreceptors UVR8 and phytochrome B cooperate to optimize plant growth and defense in patchy canopies. *New Phytologist*, 207, 4–9. Available from: https://doi.org/10.1111/nph.13332

Mehrtens, F., Kranz, H., Bednarek, P. & Weisshaar, B. (2005) The *Arabidopsis* transcription factor MYB12 is a flavonol-specific regulator of phenylpropanoid biosynthesis. *Plant Physiology*, 138, 1083–1096. Available from: https://doi.org/10.1104/pp.104.058032

Morales, L.O., Brosché, M., Vainonen, J., Jenkins, G.I., Wargent, J.J., Sipari, N. et al. (2013) Multiple roles for UV RESISTANCE LOCUS8 in regulating gene expression and metabolite accumulation in *Arabidopsis* under solar ultraviolet radiation. *Plant Physiology*, 161, 744–759. Available from: https://doi.org/10.1104/pp.112.211375

Moriconi, V., Binkert, M., Costigliolo, C., Sellaro, R., Ulm, R. & Casal, J.J. (2018) Perception of sunflecks by the UV-B photoreceptor UV RESISTANCE LOCUS8. *Plant Physiology*, 177, 75–81. Available from: https://doi.org/10.1104/pp.18.00048

Navarro, A., Bañon, S., Olmos, E. & Sánchez-Blanco, M.J. (2007) Effects of sodium chloride on water potential components, hydraulic conductivity, gas exchange and leaf ultrastructure of *Arbutus unedo* plants. *Plant Science*, 172, 473–480. Available from: https://doi.org/10.1016/j.plantsci.2006.10.006

Neugart, S., Hideg, É., Czégény, G., Schreiner, M. & Strid, Å. (2020) Ultraviolet-B radiation exposure lowers the antioxidant capacity in the *Arabidopsis thaliana* pdx1.3-1 mutant and leads to glucosinolate biosynthesis alteration in both wild type and mutant. *Photochemical & Photobiological Sciences*, 19, 217–228. Available from: https://doi.org/10.1039/c9pp00342h

Neugart, S., Rohn, S. & Schreiner, M. (2015) Identification of complex, naturally occurring flavonoid glycosides in *Vicia faba* and *Pisum sativum* leaves by HPLC-DAD-ESI-MSn and the genotypic effect on their flavonoid profile. *Food Research International*, 76, 114–121. Available from: https://doi.org/10.1016/j.foodres.2015.02.021

Neugart, S., Tobler, M.A. & Barnes, P.W. (2019) Different irradiances of UV and PAR in the same ratios alter the flavonoid profiles of *Arabidopsis thaliana* wild types and UV-signalling pathway mutants. *Photochemical & Photobiological Sciences*, 18, 1685–1699. Available from: https://doi.org/10.1039/c8pp00496j

Pescheck, F. & Bilger, W. (2019) High impact of seasonal temperature changes on acclimation of photoprotection and radiation-induced damage in field grown *Arabidopsis thaliana*. *Plant Physiology and Biochemistry*, 134, 129–136. Available from: https://doi.org/10.1016/j.plaphy.2018.07.037

Peters, K., Worrich, A., Weinhold, A., Alka, O., Balcke, G., Birkemeyer, C. et al. (2018) Current challenges in plant eco-metabolomics. *International Journal of Molecular Sciences*, 19, 1385. Available from: https://doi.org/10.3390/ijms19051385

Podolec, R. & Ulm, R. (2018) Photoreceptor-mediated regulation of the COP1/SPA E3 ubiquitin ligase. *Current Opinion in Plant Biology*, 45, 18–25. Available from: https://doi.org/10.1016/j.pbi.2018.04.018

Rai, N., Neugart, S., Yan, Y., Wang, F., Siipola, S.M., Lindfors, A.V. et al. (2019) How do cryptochromes and UVR8 interact in natural and simulated sunlight? *Journal of Experimental Botany*, 70, 4975–4990. Available from: https://doi.org/10.1093/jxb/erz236

Rai, N., O'Hara, A., Farkas, D., Safronov, O., Ratanasopa, K., Wang, F. et al. (2020) The photoreceptor UVR8 mediates the perception of both UV-B and UV-A wavelengths up to 350 nm of sunlight with responsivity moderated by cryptochromes. *Plant, Cell & Environment*, 43, 1513–1527. Available from: https://doi.org/10.1111/pce.13752

Rizzini, L., Favory, J.-J., Cloix, C., Faggionato, D., O'Hara, A., Kaiserli, E. et al. (2011) Perception of UV-B by the *Arabidopsis* UVR8 protein. *Science*, 332, 103–106. Available from: https://doi.org/10.1126/science.1200660

Robson, T.M., Klem, K., Urban, O. & Jansen, M.A.K. (2015) Re-interpreting plant morphological responses to UV-B radiation. *Plant, Cell & Environment*, 38, 856–866. Available from: https://doi.org/10.1111/pce.12374

Rodríguez, V.M., Soengas, P., Alonso-Villaverde, V., Sotelo, T., Cartea, M.E. & Velasco, P. (2015) Effect of temperature stress on the early vegetative development of *Brassica oleracea* L. *BMC Plant Biology*, 15, 145. Available from: https://doi.org/10.1186/s12870-015-0535-0

Rodríguez-Calzada, T., Qian, M., Strid, Å., Neugart, S., Schreiner, M., Torres-Pacheco, I. et al. (2019) Effect of UV-B radiation on morphology, phenolic compound production, gene expression, and subsequent drought stress responses in chili pepper (*Capsicum annuum* L.). *Plant Physiology and Biochemistry*, 134, 94–102. Available from: https://doi.org/10.1016/j.plaphy.2018.06.025

Saito, K., Yonekura-Sakakibara, K., Nakabayashi, R., Higashi, Y., Yamazaki, M., Tohge, T. et al. (2013) The flavonoid biosynthetic pathway in *Arabidopsis*: structural and genetic diversity. *Plant Physiology and Biochemistry*, 72, 21–34. Available from: https://doi.org/10.1016/j.plaphy.2013.02.001

Schmidt, S., Zietz, M., Schreiner, M., Rohn, S., Kroh, L.W. & Krumbein, A. (2010) Identification of complex, naturally occurring flavonoid glycosides in kale (*Brassica oleracea* var. sabellica) by high-performance liquid chromatography diode-array detection/electrospray ionization multi-stage mass spectrometry. *Rapid Communications in Mass Spectrometry*, 24, 2009–2022. Available from: https://doi.org/10.1002/rcm.4605

Schneider, C.A., Rasband, W.S. & Eliceiri, K.W. (2012) NIH Image to ImageJ: 25 years of image analysis. *Nature Methods*, 9, 671–675. Available from: https://doi.org/10.1038/nmeth.2089

Schreiner, M., Mewis, I., Huyskens-Keil, S., Jansen, M.A.K., Zrenner, R., Winkler, J.B. et al. (2012) UV-B-induced secondary plant metabolites - potential benefits for plant and human health. *Critical Reviews in Plant Sciences*, 31, 229–240. Available from: https://doi.org/10.1080/07352689.2012.664979

Sommer, S.G., Castro-Alves, V., Hyötyläinen, T., Strid, Å. & Rosenqvist, E. (2023) The light spectrum differentially influences morphology, physiology and metabolism of Chrysanthemum × morifolium without affecting biomass accumulation. *Physiologia Plantarum*, 175, e14080. Available from: https://doi.org/10.1111/ppl.14080

Stockenhuber, R., Akiyama, R., Tissot, N., Milosavljevic, S., Yamazaki, M., Wyler, M. et al. (2024) UV RESISTANCE LOCUS 8-mediated UV-B response is required alongside CRYPTOCHROME 1 for plant survival in sunlight under field conditions. *Plant and Cell Physiology*, 65, 35–48. Available from: https://doi.org/10.1093/pcp/pcad113

Stracke, R., Favory, J.-J., Gruber, H., Bartelniewoehner, L., Bartels, S., Binkert, M. et al. (2010) The *Arabidopsis* bZIP transcription factor HY5 regulates expression of the PFG1/MYB12 gene in response to light and ultraviolet-b radiation. *Plant, Cell & Environment*, 33, 88–103. Available from: https://doi.org/10.1111/j.1365-3040.2009.02061.x

Tissot, N. & Ulm, R. (2020) Cryptochrome-mediated blue-light signalling modulates UVR8 photoreceptor activity and contributes to UV-B tolerance in *Arabidopsis*. *Nature Communications*, 11, 1323. Available from: https://doi.org/10.1038/s41467-020-15133-y

Wangkumhang, P., Chaichoompu, K., Ngamphiw, C., Ruangrit, U., Chanprasert, J., Assawamakin, A. et al. (2007) WASP: a Web-based Allele-Specific PCR assay designing tool for detecting SNPs and mutations. *BMC Genomics*, 8, 275. Available from: https://doi.org/10.1186/1471-2164-8-275

Wargent, J.J., Gegas, V.C., Jenkins, G.I., Doonan, J.H. & Paul, N.D. (2009) UVR8 in *Arabidopsis thaliana* regulates multiple aspects of cellular

differentiation during leaf development in response to ultraviolet B radiation. *New Phytologist*, 183, 315–326. Available from: https://doi.org/10.1111/j.1469-8137.2009.02855.x

Wiesner, M., Zrenner, R., Krumbein, A., Glatt, H. & Schreiner, M. (2013) Genotypic variation of the glucosinolate profile in pak choi (*Brassica rapa* ssp. chinensis). *Journal of Agricultural and Food Chemistry*, 61, 1943–1953. Available from: https://doi.org/10.1021/jf303970k

de Wit, M., Galvão, V.C. & Fankhauser, C. (2016) Light-mediated hormonal regulation of plant growth and development. *Annual review of plant biology*, 67, 513–537. Available from: https://doi.org/10.1146/annurev-arplant-043015-112252

Di Wu, W.u, Hu, Q., Yan, Z., Chen, W., Yan, C., Huang, X. et al. (2012) Structural basis of ultraviolet-b perception by UVR8. *Nature*, 484, 214–219. Available from: https://doi.org/10.1038/nature10931

Yamasaki, H., Sakihama, Y. & Ikehara, N. (1997) Flavonoid-Peroxidase reaction as a detoxification mechanism of plant cells against H2O2. *Plant Physiology*, 115, 1405–1412. Available from: https://doi.org/10.1104/pp.115.4.1405

Yang, L., Wen, K.-S., Ruan, X., Zhao, Y.-X., Wei, F. & Wang, Q. (2018) Response of plant secondary metabolites to environmental factors. *Molecules*, 23, 762. Available from: https://doi.org/10.3390/molecules23040762

Zimmermann, N.S., Gerendás, J. & Krumbein, A. (2007) Identification of desulphoglucosinolates in Brassicaceae by LC/MS/MS: comparison of ESI and atmospheric pressure chemical ionisation-MS. *Molecular Nutrition & Food Research*, 51, 1537–1546. Available from: https://doi.org/10.1002/mnfr.200700103

## SUPPORTING INFORMATION

Additional supporting information can be found online in the Supporting Information section at the end of this article.

**How to cite this article:** Neugart, S., Steininger, V., Fernandes, C., Martínez-Abaigar, J., Núñez-Olivera, E., Schreiner, M. et al. (2024) A synchronized, large-scale field experiment using *Arabidopsis thaliana* reveals the significance of the UV-B photoreceptor UVR8 under natural conditions. *Plant, Cell & Environment*, 1–17. https://doi.org/10.1111/pce.15008